

RESEARCH ARTICLE

Developmental loss of neurofibromin across distributed neuronal circuits drives excessive grooming in *Drosophila*

Lanikea B. King¹, Tamara Boto¹, Valentina Botero¹, Ari M. Aviles^{1,2}, Breanna M. Jomsky^{1,2}, Chevara Joseph^{1,2}, James A. Walker³, Seth M. Tomchik^{1*}

1 Department of Neuroscience, The Scripps Research Institute, Jupiter, Florida, United States of America, **2** Honors College, Florida Atlantic University, Jupiter, Florida, United States of America, **3** Center for Genomic Medicine, Massachusetts General Hospital, Harvard Medical School, Cambridge, Massachusetts, United States of America

* stomchik@scripps.edu



OPEN ACCESS

Citation: King LB, Boto T, Botero V, Aviles AM, Jomsky BM, Joseph C, et al. (2020) Developmental loss of neurofibromin across distributed neuronal circuits drives excessive grooming in *Drosophila*. PLoS Genet 16(7): e1008920. <https://doi.org/10.1371/journal.pgen.1008920>

Editor: Julie Simpson, UCSB, UNITED STATES

Received: March 12, 2020

Accepted: June 8, 2020

Published: July 22, 2020

Copyright: © 2020 King et al. This is an open access article distributed under the terms of the [Creative Commons Attribution License](https://creativecommons.org/licenses/by/4.0/), which permits unrestricted use, distribution, and reproduction in any medium, provided the original author and source are credited.

Data Availability Statement: All grooming data are available in the Dryad data repository (doi:[10.5061/dryad.bvq83bk67](https://doi.org/10.5061/dryad.bvq83bk67)).

Funding: Research support was provided by NIH R01 NS097237 (S.M.T.), NIH R21 NS096402, DOD NFRP W81XWH-16-1-0220, and a generous donation from the Kanter family (J.A.W.). The funders had no role in study design, data collection and analysis, decision to publish, or preparation of the manuscript.

Competing interests: The authors have declared that no competing interests exist.

Abstract

Neurofibromatosis type 1 is a monogenetic disorder that predisposes individuals to tumor formation and cognitive and behavioral symptoms. The neuronal circuitry and developmental events underlying these neurological symptoms are unknown. To better understand how mutations of the underlying gene (*NF1*) drive behavioral alterations, we have examined grooming in the *Drosophila* neurofibromatosis 1 model. Mutations of the fly *NF1* ortholog drive excessive grooming, and increased grooming was observed in adults when Nf1 was knocked down during development. Furthermore, intact Nf1 Ras GAP-related domain signaling was required to maintain normal grooming. The requirement for Nf1 was distributed across neuronal circuits, which were additive when targeted in parallel, rather than mapping to discrete microcircuits. Overall, these data suggest that broadly-distributed alterations in neuronal function during development, requiring intact Ras signaling, drive key Nf1-mediated behavioral alterations. Thus, global developmental alterations in brain circuits/systems function may contribute to behavioral phenotypes in neurofibromatosis type 1.

Author summary

Neurofibromatosis type 1 results in increased susceptibility to cognitive and behavioral symptoms, such as attention-deficit/hyperactivity disorder. This suggests that the underlying genetic mutations affect neuronal function. Where and when these effects occur in the brain is not understood. We approached these questions in the genetically-powerful fly model, examining how loss of the *NF1* gene affects a complex motor behavior, grooming. Loss of *NF1* during brain development caused excessive grooming in adult animals. This suggests that the gene plays a key role in brain development, which may be important for treatment of the disorder. Further, we found that a specific signaling pathway, Ras, is involved in regulating this grooming behavior. Finally, we mapped where in the brain the neurofibromin (Nf1) protein is required to maintain normal levels of grooming. The data suggested that it is required across many neurons, rather than in small subsets. When Nf1

was knocked down in smaller subsets, there was no effect, but if two subsets were added together, an effect was produced. This means that Nf1 regulates the function of many neurons and brain regions to influence complex behaviors.

Introduction

Many genetic disorders affect cognitive and behavioral function in humans. Among these, neurofibromatosis type 1 (NF1) affects approximately 1 in 3000 people, making it among the most common monogenetic disorders associated with cognitive dysfunction [1,2]. While its core symptoms include neurofibromas, optic gliomas, and café au lait spots, the disorder also predisposes individuals to cognitive or behavioral symptoms such as hyperactivity, problems with attention, disrupted sleep, repetitive behaviors, and difficulty with social encounters [1–9]. Along these lines, NF1 increases risk for attention-deficit/hyperactivity disorder [1,2,6] and autism spectrum disorder [4,5,7,9,10]. These cognitive and behavioral symptoms affect quality of life and are considered major contributors to lifetime morbidity in NF1 patients [1,10,11]. NF1 is caused by a mutation in the *NF1* gene encoding the neurofibromin (Nf1) protein. Neurofibromin acts as a GTPase-activating protein (GAP) for Ras, thus reducing active Ras signaling [12–14]. In addition to this major role in Ras signaling, neurofibromin has also been implicated in G protein-coupled receptor signal transduction, modulation of cAMP levels, and dopaminergic circuit function [15–21]. These pathways modulate both developmental processes, such as cell proliferation, migration, fate specification, apoptosis, and morphology, as well as cellular physiology and plasticity in adults [22,23].

How loss of neurofibromin drives behavioral alterations, via effects on neuronal circuits, is a major question. NF1 phenotypes have been associated with a variety of cell types. For example, tumors in NF1 arise from multiple cell types: optic gliomas originate from astroglia [24], while neurofibromas originate from Schwann cells [25]. In some cases, behavioral phenotypes have been mapped to discrete neuronal populations in the brain. Learning deficits in *Nf1* mutant mice stem from the loss of the gene in GABAergic inhibitory interneurons but not excitatory neurons or glia [26]. Motor and depression-like phenotypes in a mouse model map to dopamine receptor D1 positive neurons in the striatum [27]. In *Drosophila*, *Nf1* mutants exhibit olfactory learning deficits that map to a subset of neurons in the mushroom bodies, important structures for learning and memory [28]. However, in other cases, *Nf1* mutant phenotypes map only to broader sets of cells. For instance, in flies, a *Nf1*-dependent body size phenotype maps only broadly to neurons [29]. Thus, localization, scope, and neurochemical identity of the neuronal circuit underlying cognitive and behavioral phenotypes in NF1 are variable and unclear. To understand how the loss of Nf1 affects neuronal circuits underlying motor behaviors, through development and into adulthood, the present study examines the biological underpinnings of repetitive aberrant grooming in the *Drosophila* NF1 model.

Results

The ventral nervous system is a major locus of Nf1-sensitive grooming circuits

Adult flies bearing *Nf1* loss of function mutations and RNAi knockdown exhibit excessive spontaneous grooming, reflecting an increase in grooming frequency and duration, due to loss of Nf1 in neurons [30]. The fly central nervous system (CNS) consists of a central brain and a ventral nervous system (VNS) that, like the mammalian spinal cord, is necessary for nearly all

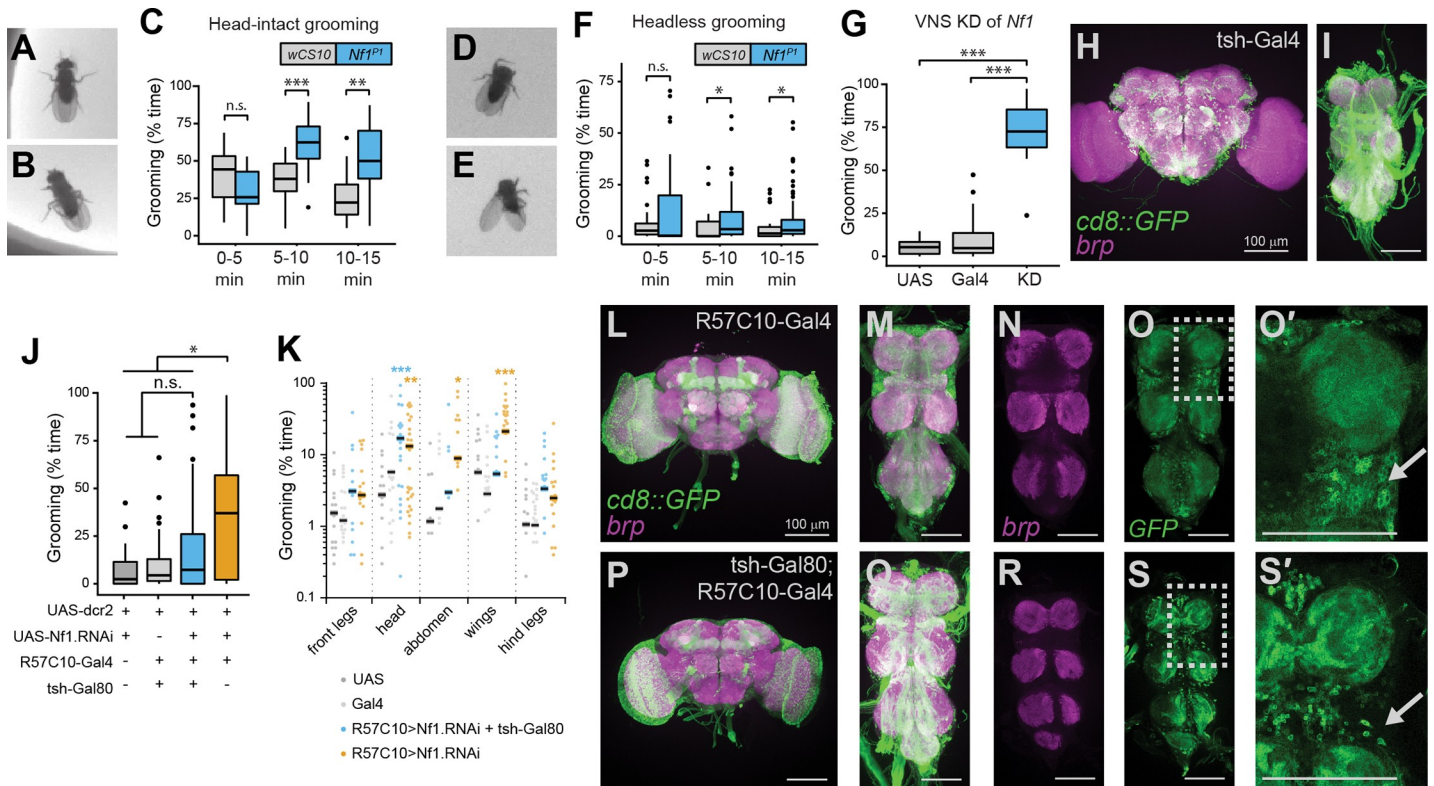


Fig 1. Neurons in the brain and ventral nervous system that modulate grooming are sensitive to loss of Nf1. (A) An intact fly grooming its anterior (prothoracic) legs. (B) An intact fly grooming its posterior (metathoracic) legs. (C) Grooming duration in intact *Nf1^{P1}* vs. *wCS10* control flies at 0, 5, and 10 min after introduction to the chamber. $n = 18$; ** $p < 0.01$, *** $p < 0.001$ (Wilcoxon rank-sum test). (D) Grooming movement directed toward the anterior body (missing head) in a decapitated fly. (E) A headless fly grooming its hind (metathoracic) legs. (F) Grooming duration in decapitated flies. $n = 25-26$; * $p < 0.05$ (Wilcoxon rank-sum test). (G) Grooming duration in flies with Nf1 knockdown in *tsh-Gal4*+ neurons. $n = 16$; $p < 0.001$ (Kruskal-Wallis); *** $p < 0.001$ (Dunn/Sidak). (H) Maximum-intensity projection showing *tsh*>UAS-mCD8::GFP (green) and bruchpilot (*brp*; magenta) in the central brain. Scale bar = 100 μ m. (I) VNS expression of *tsh* and *brp*, as in panel H. (J) Grooming duration with pan-neuronal knockdown (KD) of Nf1 via the R57C10-Gal4, with or without the *tsh-Gal80* repressor. $n = 40-42$; $p < 0.001$ (Kruskal-Wallis); * $p < 0.05$ (Dunn/Sidak). (K) Grooming duration from the same data set in panel J, graphed by body part groomed. Individual data points are graphed (zero values are not plotted), with the mean shown as a line. Stars represent significance re: UAS control. (L) Maximum-intensity projection of anti-GFP (green) and anti-*brp* (magenta) immunostaining in the central brain of an R57C10-Gal4 > UAS-mCD8::GFP fly. Scale bar = 100 μ m. (M) R57C10-Gal4 expression pattern in the VNS, imaged as in panel K. (N) Single z-plane showing anti-*brp* neuropil staining from the VNS in panel L. (O) GFP staining from the VNS plane in panel L. (O') Expanded detail from the dashed box in panel N. Arrow points to area of dense somata. (P) Maximum-intensity projection of the brain of an R57C10-Gal4 > UAS-mCD8::GFP, UAS-*tsh-Gal80* fly. (Q) Expression pattern in the VNS of the same fly shown panel K. (R) Single z-plane showing anti-*brp* neuropil staining from the VNS in panel P. (S) GFP staining from the VNS plane in panel Q. (S') Expanded detail from the dashed box in panel N. Arrow points to area of reduced somata density by *tsh-Gal80* repression.

<https://doi.org/10.1371/journal.pgen.1008920.g001>

motor output. To gain insight into the neuronal circuits mediating this increase in grooming, we first parsed the roles of neurons in the brain from those in the VNS. Descending neurons send projections from the brain to the VNS and initiate a range of behaviors including grooming [31–33]. To test whether loss of Nf1 increased grooming via neurons originating in the brain, we decapitated *Nf1^{P1}* mutants and observed grooming in an open field. *Nf1^{P1}* mutants harbor a large deletion in the *NF1* locus and express no functional protein [16]. Because decapitation requires anesthesia, we first tested whether intact flies groom normally after anesthesia. Normal grooming behaviors were observed after anesthesia, including grooming of the head (Fig 1A) and abdomen (Fig 1B). As previously reported [34,35], decapitated flies survive until desiccated and typically stand still or groom. During the first five minutes after transfer to an open field chamber, *Nf1^{P1}* mutants and genetic controls groomed at indistinguishable durations (Fig 1C). However, after 5 min of acclimation to the open field, *Nf1^{P1}* mutants groomed significantly longer than controls (Fig 1C). This is consistent with previous results in which

Nf1 mutants groomed more than control flies after an acclimation period [30]. In addition to grooming intact posterior body parts (Fig 1E), decapitated flies made grooming-like front leg sweeps toward the location of the missing head, suggesting that the head grooming motor pattern can be activated in the absence of the actual head and brain (Fig 1D). Similar to intact animals, decapitated *Nf1* mutants and genetic controls groomed for equivalent durations during the first 5 minutes in the open field (Fig 1F). However, after acclimation, decapitated *Nf1* mutants exhibited a significant increase in grooming relative to genetic controls (Fig 1F). Thus, overall, *Nf1* mutants exhibited elevated levels of grooming in the absence of a central brain, preliminarily pointing toward VNS circuits as a major locus of *Nf1* sensitivity.

To further test the role of *Nf1* in VNS circuits with a genetic approach, we turned to the Gal4/UAS system and RNAi-mediated knockdown of *Nf1* [36]. Using the *tsh*-Gal4 driver [37] to knock down *Nf1* preferentially in the VNS, we observed significantly elevated grooming compared to genetic controls (Fig 1G). To validate the VNS specificity of *tsh*-GAL4, we used the driver to express UAS-mCD8::GFP and found relatively sparse expression of GFP in the brain (Fig 1H) and widespread labeling of neuropil and cell bodies in the VNS (Fig 1I). We next used the converse approach to determine whether VNS knockdown of *Nf1* is necessary for excessive grooming, using a *tsh*-GAL80 transgene to subtract a subset of VNS neurons that would otherwise be targeted by a pan-neuronal driver. Flies that were spared *Nf1* knockdown in the VNS groomed significantly less than pan-neuronal *Nf1* knockdown flies—their total grooming did not significantly differ from genetic controls lacking the driver or effectors (Fig 1J). However, analysis of the grooming of individual body parts revealed a more nuanced picture. Pan-neuronal knockdown significantly increased grooming of the head, abdomen, and wings (Fig 1K). Addition of the *tsh*-Gal80 transgene eliminated this excess grooming in the wings and abdomen, suggesting that the localization of *Nf1*-sensitive neurons driving wing and abdomen grooming is biased toward the VNS. However, head grooming remained elevated (Fig 1K), suggesting that some of the *Nf1*-sensitive neurons driving head grooming localize to the brain. Using immunohistochemistry, we compared brain and VNS labeling of R57C10-Gal4 (Fig 1L and 1M) and *tsh*-GAL80;R57C10-Gal4 (Fig 1P and 1Q). We observed a loss of VNS cell body staining in flies carrying *tsh*-GAL80 (Fig 1S) compared to pan-neuronal R57C10-Gal4 labeling (Fig 1O), consistent with previous observations [38]. Together, these results suggest that *Nf1*-sensitive grooming circuits are distributed across both the brain and VNS, with the VNS being a key site for *Nf1*-sensitive grooming neurons.

Neurochemical identity of *Nf1*-sensitive grooming neurons

To determine whether any major cell types are differentially associated with the excessive grooming phenotype, we knocked down *Nf1* in defined neuronal subsets. A driver previously associated with a *Nf1* body size phenotype, 69B-Gal4 [29], increased grooming when used to knock down *Nf1* (Fig 2A). This driver labels the brain sparsely (Fig 2B) and the VNS more strongly (Fig 2C). Knocking down *Nf1* in cholinergic neurons, the primary excitatory neuronal population in the fly nervous system, with ChAT-Gal4 also resulted in excessive grooming compared to genetic controls (Fig 2G). This driver labels neurons broadly across the brain (Fig 2H) and VNS (Fig 2I). In contrast, knockdown of *Nf1* in neurons expressing the other major neurotransmitters GABA (*Gad1*-Gal4) or glutamate (*vGluT*-Gal4) did not produce any differences in grooming (Fig 2J and 2K). Likewise, *Nf1* knockdown in dopaminergic neurons using TH-Gal4 did not influence grooming behavior (Fig 2L). However, the oct-tyrR-Gal4 [39] driver that labels a subset of neurons that express the oct-tyrR receptor, produced excessive grooming when used to knock down *Nf1* (Fig 2D). This driver labels a broadly-distributed but relatively sparse population of neurons in the brain (Fig 2H) and VNS (Fig 2I). The oct-tyrR

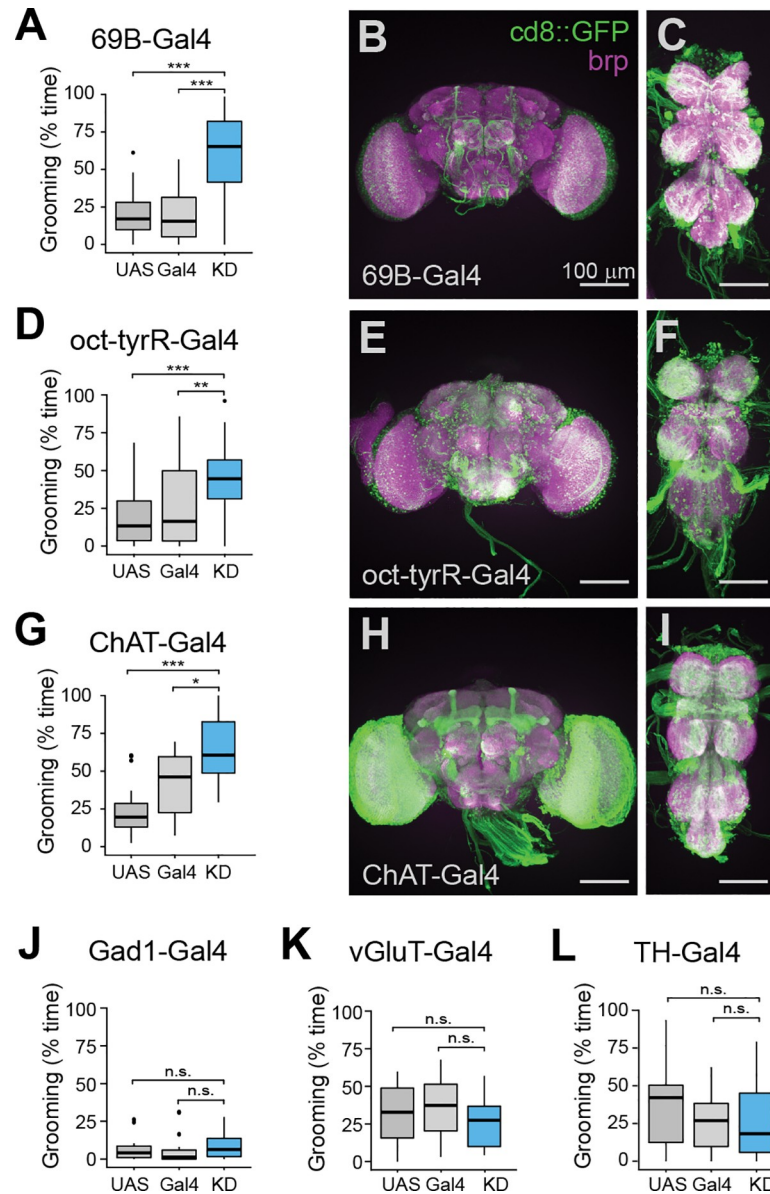


Fig 2. Loss of Nf1 in broad sets of excitatory neurons increases grooming. (A) Grooming duration with Nf1 knockdown (KD) in 69B-Gal4⁺ neurons. $n = 20$; $p < 0.001$ (Kruskal-Wallis). (B) Maximum-intensity projection of 69B-Gal4 expression (green) and anti-brp immunostaining (magenta) in the brain. Scale bar = 100 μ m. (C) VNS expression of 69B as in panel B. (D) Knockdown of Nf1 in oct-tyrR-Gal4⁺ neurons. $n = 20$; $p < 0.001$ (Kruskal-Wallis). (E) Brain expression of the oct-tyrR-Gal4 driver. (F) VNS expression of the oct-tyrR-Gal4 driver. (G) Knockdown of Nf1 using the ChAT-T2A-Gal4 driver. $n = 20$; $p < 0.001$ (Kruskal-Wallis). (H) Brain expression of the ChAT-T2A-Gal4 driver. (I) VNS expression of the ChAT-T2A-Gal4 driver. (J) Knockdown of Nf1 in Gad1-Gal4⁺ neurons. $n = 18$ each; $p = 0.23$ (Kruskal-Wallis). (K) Knockdown of Nf1 in vGluT-Gal4⁺ neurons. $n = 20$; $p = 0.45$ (Kruskal-Wallis). (L) Knockdown of Nf1 in TH-Gal4⁺ neurons. $n = 20$; $p = 0.6$ (Kruskal-Wallis). * $p < 0.05$, ** $p < 0.01$, *** $p < 0.001$ (Dunn/Sidak).

<https://doi.org/10.1371/journal.pgen.1008920.g002>

receptor responds to both octopamine and tyramine [40], suggesting that monoaminergic sensitive oct-tyrR⁺ neurons may be a Nf1-sensitive population that regulates grooming levels. Collectively, these data suggest that the population of neurons associated with elevated grooming is broadly distributed, biased toward the VNS, excitatory, cholinergic, and oct-tyrR⁺.

Excessive grooming involves the Nf1 GAP-related domain

The most well-described biochemical function of Nf1 is its conserved Ras-GAP activity, inhibiting Ras [12,41]. However, it also affects other signaling cascades via direct and putative indirect interactions, such as G protein-coupled receptor signaling and cAMP/PKA regulation [16,17,19,27,42–46]. To begin probing the critical downstream effectors regulating the grooming phenotype, we used the Gal4-UAS system to express wild-type and GAP-related domain (GRD) mutant Nf1 transgenes in an *Nf1* mutant background. For this experiment, we used a heteroallelic *Nf1*^{P1}/*Nf1*^{E1} mutant. The *Nf1*^{E1} allele is a nonsense mutation that truncates the protein upstream of the GRD [29]. This heteroallelic combination, chosen to circumvent lethality of the E1 mutation and facilitate introduction of transgenic rescue constructs, exhibited excessive grooming, similar to the homozygous *Nf1*^{P1} mutants and pan-neuronal Nf1 RNAi (Fig 3B). In this background, we pan-neuronally expressed either a wild-type Nf1 transgene (Fig 3A) or one containing a point mutation (R1320P) in the Ras GAP-related domain (GRD), which impairs its catalytic activity (Fig 3A). The R1320P mutation is modeled on the orthologous human neurofibromatosis 1 patient-derived R1276P mutation. This mutation in the “arginine finger” of the GRD prevents Nf1 from binding Ras and reduces GAP activity >8000 fold [29,47]. Expressing the wild-type Nf1 transgene reduced grooming to control levels (Fig 3B). However, the Nf1^{R1320P} transgene failed to rescue, as flies expressing it groomed

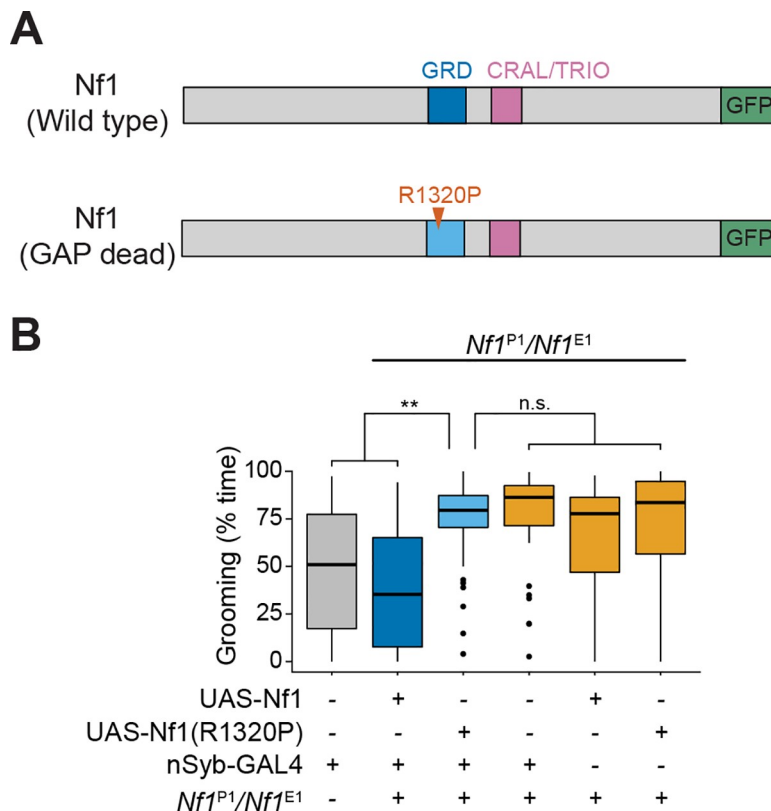


Fig 3. Functional Nf1 GAP-related domain (GRD) is required to maintain normal grooming frequency. (A) Diagram of the wild type (top) and mutated (bottom) Nf1 rescue constructs. Major protein domains, the R1320P mutation, and GFP C-terminal fusions are depicted. (B) Grooming durations for (left to right): (1) nSyb-Gal4 genetic control, and *Nf1*^{P1}/*Nf1*^{E1} mutants expressing (2) wild-type UAS-Nf1 rescue, (3) UAS-Nf1^{R1320P} rescue, (4) nSyb-Gal4 alone, (5) UAS-Nf1 alone, and (6) UAS-Nf1^{R1320P} alone. n = 40; p < 0.001, Kruskal-Wallis; **p < 0.01, n.s.: not significant (Dunn/Sidak).

<https://doi.org/10.1371/journal.pgen.1008920.g003>

significantly more than both wild-type controls and flies expressing the wild-type rescue construct (Fig 3B). Thus, the ability of Nf1 to regulate Ras is crucial to maintaining normal grooming activity.

Nf1 regulates adult grooming via a developmental critical window

To determine whether excessive grooming reflects developmental effects or an ongoing requirement for Nf1 in adult neurons, we used the Gal80^{ts} conditional expression system [48]. A ubiquitously expressed temperature-sensitive GAL80 (tub-GAL80^{ts}) was used to control Gal4-UAS activity driving Nf1 RNAi. We first raised embryos or larvae at the permissive temperature (18°C) to prevent GAL4/UAS-mediated Nf1 knockdown during development, and subsequently placed the eclosed adults at the restrictive temperature (30°C), knocking down Nf1 only during adulthood. Adult-specific Nf1 knockdown did not produce a significant effect on grooming (Fig 4G). In contrast, conditional knockdown of Nf1 during the late larval (3rd instar) and pupal stages (Fig 4B), but not early development (through 2nd instar) (Fig 4A), produced excessive grooming in adulthood. Reducing the duration of Nf1 knockdown, we found that knockdown during the pupal stage caused significantly higher levels of grooming over genetic controls (Fig 4D), whereas knockdown during only the 3rd instar larval stage did not significantly change grooming from both genetic controls (Fig 4C). Subdividing Nf1 knockdown within the pupal stage into halves produced no significant effect, relative to both controls, in either half (Fig 4E and 4F). Therefore, we conclude that the pupal stage is a critical developmental window when Nf1 is required for the development of circuits that maintain appropriate levels of grooming activity in adults.

Developmental pattern of Nf1-sensitive neurons during the pupal stage

Among the Gal4 lines that produced an increase in grooming when knocking down Nf1, the oct-tyrR-Gal4 labels a neurochemically discrete population of neurons, which have been associated with locomotor control [49,50]. Gal4 expression patterns can shift during development [51]. As Nf1 is expressed broadly in the nervous system [29], this opens at least two potential mechanisms for the developmental regulation of grooming: the phenotype could be due to dynamic knockdown of Nf1 caused by changes in driver expression over time, or the cellular requirement for Nf1 could change over time despite relatively stable RNAi expression. To discriminate between these possibilities, we examined the expression patterns of the oct-tyrR-Gal4 driver during the pupal stage. Using immunohistochemistry, we visualized oct-tyrR+ neurons at the beginning (Fig 5A), middle (Fig 5B and 5C), and end (Fig 5D and 5E) of the pupal stage. oct-tyrR+ neurons were well represented throughout development and broadly innervate neuropil in the brain and VNS.

Additive influence of microcircuits is required to express hyperactive grooming

To test smaller subsets of neurons for sensitivity to Nf1 knockdown, we screened a subset of 212 genomic enhancer-driven Gal4 lines that exhibit sparse expression in the VNS [52]. In an initial screen, each Gal4 line was used to knock down Nf1 and grooming was scored (n = 10 each). These lines exhibited a range of grooming frequencies, from nearly zero to over 50% median time spent grooming (S1 Fig). The lines with the highest absolute grooming frequencies (> 40%) were selected for follow-up testing, which involved comparing the knockdown genotype (Gal4>UAS-Nf1) with two genetic controls (Gal4/+ and UAS-Nf1/+). None of the lines selected for follow-up testing exhibited grooming significantly and consistently elevated relative to both controls (S2 Fig). Among lines that did not reach threshold for follow-up were

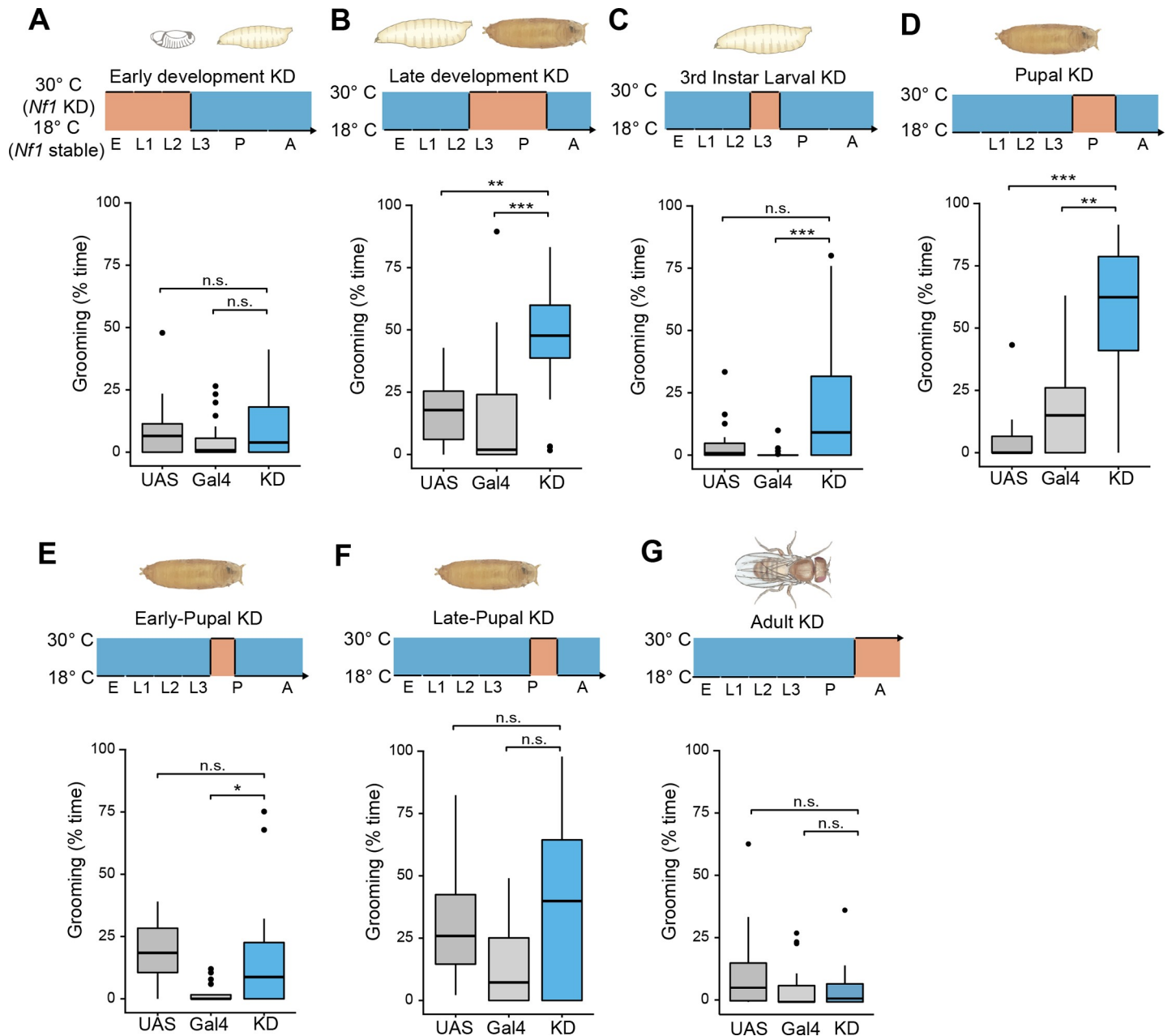


Fig 4. Excessive grooming results from the loss of Nf1 during a critical developmental window. Gal80^{TS} was used to restrict knockdown (KD) of Nf1 with RNAi to different time windows during development and adulthood. (A-G) In each panel, elav-Gal4 > UAS-Nf1 RNAi, tub-Gal80^{TS} (knockdown [KD]) is compared to UAS-Nf1 RNAi (UAS) and elav-Gal4 and tub-Gal80^{TS} (Gal4) controls. n = 20. *p < 0.05, **p < 0.01, ***p < 0.001 (Dunn-Sidak). (A) Knockdown during embryo through larval L2 stage. p = 0.37 (Kruskal-Wallis). (B) Larval L3 and pupal stages. p < 0.001 (Kruskal-Wallis). (C) Larval L3 stage. p < 0.001 (Kruskal-Wallis). (D) Pupal stage. p < 0.001 (Kruskal-Wallis). (E) Early pupal stage. p < 0.001 (Kruskal-Wallis). (F) Late pupal stage. p = 0.05 (Kruskal-Wallis). (G) Knockdown in adulthood, following eclosion. p = 0.1 (Kruskal-Wallis).

<https://doi.org/10.1371/journal.pgen.1008920.g004>

lines that express in sensory neurons across the body and have been previously shown to elevate grooming when stimulated (R52A06-, R30B01-, and R81E10-GAL4) [35]. They did not recapitulate the excessive grooming phenotype when used to knock down Nf1 (S1 Fig). Similarly, several other neuronal subsets that drive grooming when stimulated (R53A06 and R50B07: wing grooming, R23A07: eye/head grooming) [53], did not recapitulate the pan-

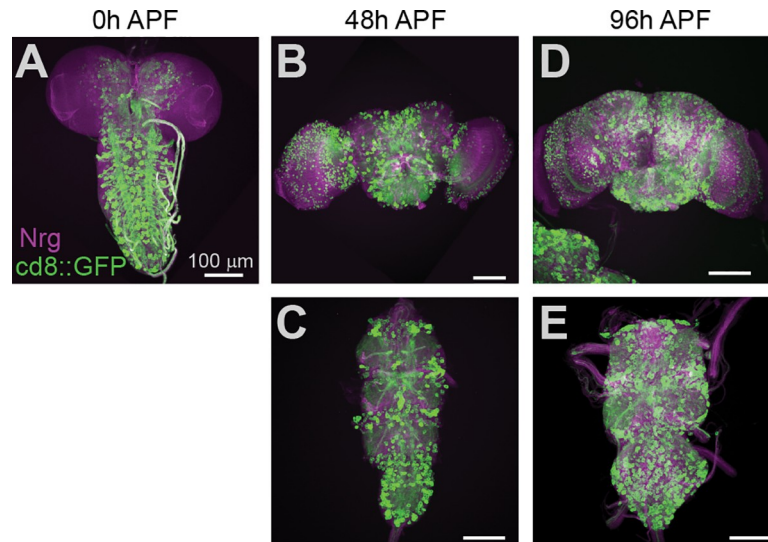


Fig 5. Octopamine-tyramine receptor+ cells are abundant throughout development. (A) Maximum-intensity projection of oct-tyrR+ neurons (green) and anti-neuroglial (Nrg) (magenta) immunostaining in the 0-hr pupal nervous system. (B) 48-hr pupal brain. (C) 48-hr pupal VNS. (D) 96-hr pupal brain. (E) 96-hr pupal VNS. APF: after puparium formation.

<https://doi.org/10.1371/journal.pgen.1008920.g005>

neuronal Nf1 phenotype (S1 Fig). Thus, elevated grooming was only observed when knocking down Nf1 with drivers that exhibit broad expression patterns: pan-neuronal, 69B, ChAT, and oct-tyrR. We cannot rule out the possibility that our screen missed a particular sparse set of neurons that would have produced a strong phenotype. Nonetheless, we reasoned that Nf1 may be required across distributed neurons for the development of normal grooming patterns, and consequently, knocking Nf1 down in more restricted neuronal subsets was insufficient to recapitulate the phenotype. If this was the case, some of the sparsely-labeled lines from our screen would be expected to function additively, further elevating grooming frequency when combined.

To test whether subsets of neurons produced additive effects, we combined pairs of Gal4 drivers. Four pairs were selected (S2 Fig) based on their relatively high levels of grooming (albeit not significant relative to controls) and nonoverlapping expression patterns [52]. Among these, two pairs of Gal4 drivers, R13F10+R11B06 and R13F10+R42A08, significantly elevated grooming when combined to knockdown Nf1 (Fig 6A and S2 Fig). Midway through the pupal stage, R13F10 and R11B06 each label a sparse set of neurons that innervate the brain and VNS neuropil in a restricted pattern (Fig 6B–6D). Doubling the dosage of a single Gal4 driver (R13F10) did not increase grooming, suggesting that the addition of the new elements from the R11B06-Gal4 driver, rather than an increase in the Gal4 dosage within the same neurons (S2 Fig), produced the effect. Neuron-glia interactions are a possible cross-cell-type interaction that could produce effects on behavior. We tested this by combining knockdown the pan-glial driver repo-Gal4 with R13F10-Gal4, and this combination failed to produce significant grooming (S2 Fig). Overall, these data suggest that the requirement for Nf1 is distributed relatively broadly across neuronal circuits, with smaller subsets producing sub-threshold, additive effects.

Discussion

The present results suggest that loss of Nf1 elevates grooming via effects during a developmental critical window, through actions that require the GAP-related domain, and via distributed

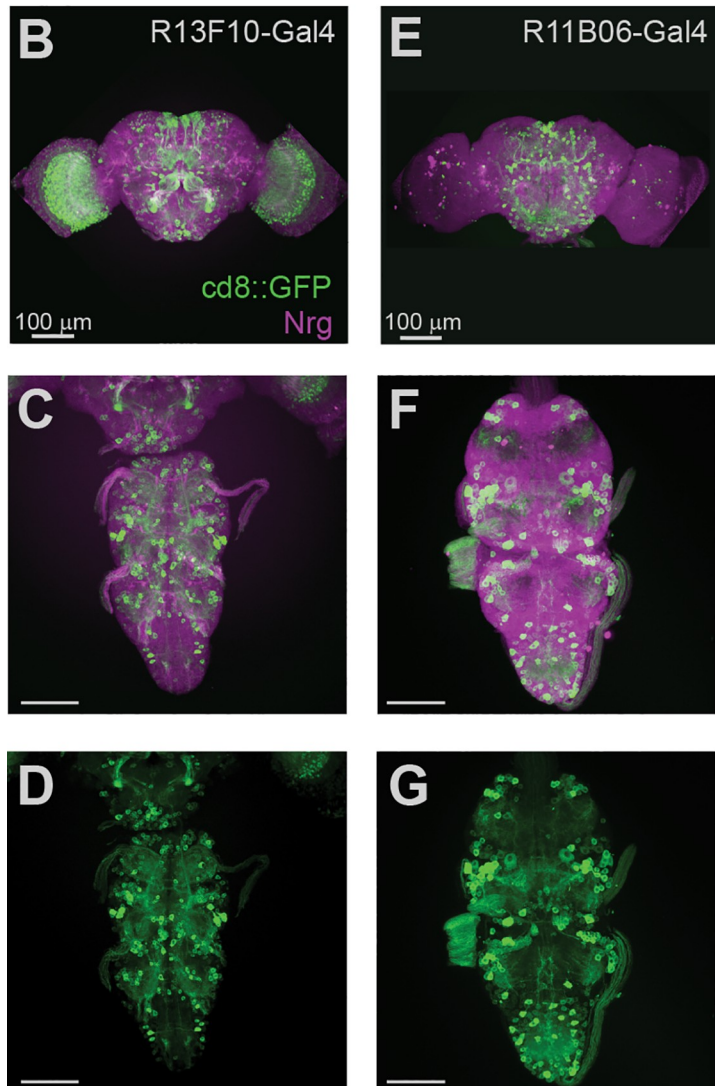
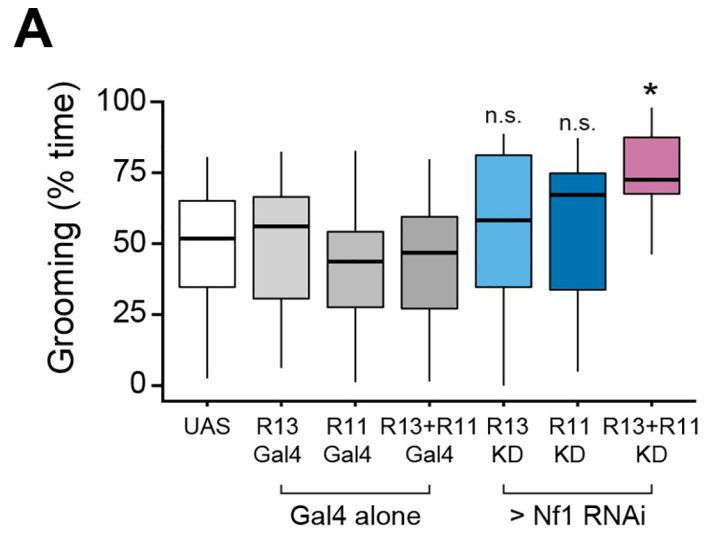


Fig 6. Loss of Nf1 across combinations of distributed circuits drives elevated grooming. (A) Grooming duration in flies with Nf1 knockdown in one or both sets of neurons labeled by the R13F10 (R13) and R11B06 (R11) Gal4 drivers. $n = 20$; Kruskal-Wallis; * $p < 0.05$ compared to UAS and Gal4 controls, n.s. not significant compared to UAS or Gal4 controls (Dunn/Sidak). (B) Maximum-intensity projection showing the expression of R13F10-Gal4 (green) and anti-neuroglian immunostaining (magenta) in a 48-hr pupal brain. (C) 48-hr pupal VNS, as in panel B. (D) GFP channel of VNS shown in panel C. (E) Maximum-intensity projection showing the expression of R11B06-Gal4 (green) and anti-neuroglian immunostaining (magenta) in a 48-hr pupal brain. (F) 48-hr pupal VNS, as in panel B. (G) GFP channel of the VNS shown in panel F.

<https://doi.org/10.1371/journal.pgen.1008920.g006>

cholinergic/oct-tyrR+ neurons. The requirement for Nf1 occurred during the pupal stage, suggesting that a distributed set of neurons may depend on Nf1 function during the formation and refinement of the adult nervous system. Oct-tyrR+ neurons are abundant during this developmental stage, though we did not explicitly test the developmental contributions of this neuronal subset in isolation. Several lines of evidence suggest that the requirement for Nf1 in order to maintain normal grooming levels is biased toward VNS neurons, including decapitation experiments, as well as tsh-Gal4/Gal80. One caveat is that the tsh-Gal4 driver exhibits expression in some neurons in the central brain (as well as the VNS). The decapitation experiments mitigate this caveat. While decapitated flies groom less than intact flies overall, decapitated *Nf1* mutants groom more than decapitated controls.

Development of the nervous system involves many important steps that are subject to plasticity, particularly during the pupal stage in *Drosophila*. During metamorphosis, neurons in the CNS exhibit dramatic changes, including programmed cell death, neurogenesis and proliferation, and neurite remodeling [54–56]. For example, connectivity between mushroom body Kenyon cells (KC) and presynaptic GABAergic neurons is dependent on pruning initiation from the post-synaptic γ KCs [57]. Losing Nf1 function could influence similar developmental processes in other parts of the nervous system and influence the development of grooming behaviors. Given the temporal resolution of the rescue experiments, our data do not rule out a dynamic role for Nf1 signaling in adult grooming, but strongly implicate developmental processes. Future studies into the developmental roles of Nf1 will be necessary to determine precisely how it influences the formation and function of neuronal circuits in the CNS, including those mediating grooming behaviors.

The requirement for intact GAP-related domain functionality suggests that Nf1-mediated Ras signaling is important for the development of normal grooming. As explored above, several critical neural developmental events occur during metamorphosis [54,55]. Ras signaling may affect these processes by acting downstream of receptor tyrosine kinases, some of which play key roles in development [58]. For instance, the receptor tyrosine kinase Alk and its ligand Jeb modulate multiple developmental processes, including patterning visceral muscle founder cells [59], mediating retinal axon targeting during metamorphosis [60], and shaping synaptic morphology and function at the neuromuscular junction [61,62]. Alk and Jeb are key genetic modifiers of the Nf1 body size/growth phenotype [63], and Nf1 mutants exhibit overgrown neuromuscular junction synapses [46]. Developmental effects of Ras have been particularly well-studied in the eye, where it modulates cell (photoreceptor) specification during metamorphosis [58,64]. Overall, this suggests that Nf1/Ras-related signaling is positioned to influence a range of developmental processes, particularly during metamorphosis.

We found that Nf1-sensitive neuronal elements modulating grooming were distributed and additive. Excessive grooming in Nf1 loss of function emanated from cholinergic (excitatory), oct-tyrR+ circuits, with VNS circuits playing a key role. The phenotype required knocking down Nf1 from across broad circuits, or combinations of smaller subsets. This contrasts with neuronal activation studies, in which some individual grooming behaviors have been mapped to small subcircuits, each driving grooming of a specific body part [31,53]. For instance, in the

antennal grooming circuit, mechanosensory neurons innervate a command circuit consisting of layered excitatory and inhibitory neurons with varying reciprocal or feed-forward connections. Optogenetic stimulation of the excitatory neurons in this command circuit drives antennal grooming [31,35]. Other body part-specific command circuits likely exist at varying locations in the nervous system, particularly in the VNS, where the majority of peripheral somatosensory neurons provide input from the peripheral nervous system. We suggest that loss of Nf1 produces sub-threshold dysfunction across multiple grooming-involved neurons and that when enough of these neurons have lost Nf1, this additive influence results in behavioral deficits. We tested 212 Gal4 lines that label restricted sets of neurons for possible Nf1-dependent effects on grooming. None of these lines elevated grooming when used alone. Interestingly, we identified two pairs of drivers that elevated grooming when combined. Future studies will evaluate whether interactions between the identified pairs of circuits or the mere addition of Nf1 loss across a critical number of neurons are factors in the development of grooming hyperactivity.

The present data demonstrate a developmental, disease-relevant behavioral phenotype in a highly tractable genetic model organism. Neurodevelopmental disorders such as NF1 often involve complex alterations in cellular signaling and complex pathophysiology. These disorders emerge early in development and may involve both dysregulations of developmental processes and alterations in acute signaling/neuronal function in the developed nervous system. Nf1 has been observed to have important functions in adult mice and flies [14,19,27,28], and some phenotypes can be rescued by acute pharmacological treatment in adult animals [65]. Nonetheless, our data suggest that Nf1 loss disrupts a distributed set of microcircuits during a critical developmental window. Thus, Nf1 acts via pleiotropic mechanisms in the cellular signaling context (influencing broad signaling cascades including Ras and cAMP/PKA) to affect distributed neuronal circuits during development and adulthood. The *Drosophila* grooming model will enable future studies to pinpoint how the loss of Nf1 dysregulates distributed neuronal networks to produce behavioral deficits in adulthood.

Materials and methods

Fly strains

Flies were raised on cornmeal/agar food medium according to standard protocols. They were housed in incubators maintained at 25°C, 60% relative humidity, and kept on a 12:12 light:dark cycle. Male flies were used for all experiments. The *Nf1*^{P1} mutation was backcrossed for 6 generations into the *wCS10* genetic background. The *Nf1*^{E1} mutation was backcrossed for 6 generations into the *w;iso2;iso3* genetic background. In experiments with mixed genetic backgrounds (e.g., *Nf1*^{P1}/*Nf1*^{E1}), control groups were background matched. The R1320P mutation was created in a wild-type cDNA using the Q5 Site-Directed Mutagenesis Kit (New England Biolabs). Wild-type and R1320P mutant Nf1 were then subcloned into the pUAST-attB vector with an in-frame C342 terminal fusion with eGFP cDNA. Transgenic lines were produced by integrating the constructs at the attP40 site (Rainbow Transgenic Flies Inc.). The Nf1 RNAi line was obtained from the Vienna *Drosophila* RNAi Center (VDRC #109637) [36] and UAS-dicer2 was used in all crosses to enhance the RNAi effect. The empty attP control line (VDRC #60100) was used in Gal4/+ control crosses to ensure a matched genetic background across all groups. The following Gal4 lines were used in this study: nSyb-Gal4, elav-Gal4, and tub-Gal80^{ts} (gifts from Ronald L. Davis), tsh-Gal80 (gift from Julie Simpson), the following lines from the Bloomington *Drosophila* Stock Center (BDSC): TH-Gal4 (BDSC# 8848), 69B-Gal4 (1774), ChAT-T2A-Gal4 (60317), Gad1-Gal4 (51630), VGluT-T2A-Gal4 (60312), tsh-Gal4 (3040), R57C10-Gal4 (nSyb; 39171), R13F10 (48578), R11B06-Gal4 (48287), R42A08-Gal4

(50144), and other Gal4 lines from the FlyLight collection were used in the VNS screen (S1 Table). Immunostaining experiments were performed using flies expressing UAS-mCD8::GFP (BDSC #32195).

Behavioral experiments

Grooming behavior experiments were performed as previously described [30]. The grooming chamber was an open field, 2.85 mm in height and 25.4 mm in diameter, consisting of an opaque (white) acrylic lateral boundary covered on the top and bottom with two clear polycarbonate sheets. The apparatus was illuminated from below with white LEDs that were filtered through a sheet of white acrylic; light intensity was measured at 720 lux in the location of the fly. Monochrome firefly MV 1394a or color firefly MV USB cameras fitted with Fujinon YV2.8×2.8SA-2 lenses were mounted above the arena. A single male fly was placed in each arena with an aspirator and recorded at 7.5 frames per second, 640 x 480 with Motion JPEG 2000 compression. Two or three videos were recorded for each subject, one immediately after loading into the chamber (0–5 min), a second at 5–10 minutes (in some experiments), and one at 15–20 min. Manual scoring of videos was carried out by an observer blind to the genotype. Start and stop frames were noted for each grooming event, which was further categorized according to which body part the fly was grooming: front legs, head/eye, abdomen, wings, or hind legs. The percentage of time spent grooming was calculated for either all events summed or individual body parts.

Immunostaining

Nervous systems of pupae 0, 48, or 96 hours after pupal formation or adult flies 5–7 days old were dissected in 1% paraformaldehyde in S2 medium, and processed according to a published protocol [52]. Brains and ventral nervous systems were incubated with the primary antibodies for 3 hours at room temperature and at 4°C overnight, and with the secondary antibodies for 3 hours at room temperature and 4 days at 4°C. Incubations were performed in blocking serum (3% normal goat serum). Labeled brains were mounted in vectashield media. Antibodies used were rabbit anti-GFP (1:1000, Invitrogen), mouse anti-brp (nc82) (1:50, DSHB), mouse anti-neuroglian (1:50, DSHB), goat anti-rabbit IgG and goat anti-mouse IgG (1:800, Alexa 488 or Alexa 633 respectively, Invitrogen). Images were obtained using Leica TCS SP8 confocal microscope.

Statistics

Normality of data was assessed with the Shapiro-Wilk Normality Test. Box plots graph the median as a line, the interquartile range (IQR) as a box, and whiskers extend to the largest value no further than 1.5xIQR; data beyond the whiskers are plotted individually as outliers. Hypothesis testing was carried out using the Wilcoxon rank-sum test (non-parametric) or Kruskal-Wallis omnibus test followed by Dunn's test with Sidak correction for multiple comparisons (non-parametric). Two-way comparisons were carried out with a two-way ANOVA, followed by Tukey's multiple comparisons tests. Statistics and graphing were performed with R version 3.2.3 with the ggplot2 package and Graphpad Prism.

Supporting information

S1 Fig. (A) Box plots showing grooming duration at the four indicated time points for flies with Nf1 knockdown using nSyb-Gal4 > Nf1 RNAi (nSyb>KD) or genetic controls with only UAS-Nf1. RNAi (UAS). n = 10; *, p < 0.05, ***, p < 0.001, Wilcoxon rank-sum test. (B)

Box plots showing grooming duration for flies with Nf1 knockdown, scored at the 5–10 min time interval, with a variety of GAL4 drivers. Lines are ranked in order of ascending median grooming duration. A cutoff threshold of 40% for follow up evaluation is indicated by a dashed red line. Gal4s are listed in [S1 Table](#).

(TIF)

S2 Fig. Follow-up behavioral experiments for putative screen hits. All panels show box plots of grooming duration for the knockdown (KD) group compared to UAS- and Gal4-only or additional controls. Grooming was scored 15–20 min after introduction to chamber. (A-I) Individual Gal4 KD. n = 20; n.s., not significant, *p < 0.05, **p < 0.01 (Dunn/Sidak). (J) An additive combination of R13F10-Gal4 and R11B06-Gal4 compared to UAS, R13F10-Gal4-only, heterozygotes of R13F10-Gal4 used for KD, homozygotes of R13F10-Gal4 used for KD, and a combination of R13F10-Gal4 with the pan-glial driver repo-Gal4. n = 20; in comparison to UAS and Gal4-only controls: n.s., not significant, ***p < 0.001 (Dunn/Sidak). (K-L) Knockdown of Nf1 using an additive combination of R13F10-Gal4 with one other Gal4, compared to UAS, doubled Gal4s (2x Gal4), and single Gal4 knockdown controls. n = 20; in comparison to UAS and 2x Gal4-only controls: n.s., not significant, ***p < 0.001 (Dunn/Sidak).

(TIF)

S1 Table. Median and first and third quartiles for each Gal4 line used in the screen shown in S1 Fig.

(XLSX)

Acknowledgments

The authors thank Ronald L. Davis and Julie Simpson for sharing fly lines, as well as Andrew Seeds, Stephanie Hampel, and Claire McKellar for helpful discussions. Stocks obtained from the Bloomington Drosophila Stock Center (NIH P40OD018537) were used in this study. Transgenic fly stocks were obtained from the Vienna Drosophila Resource Center (VDRC, www.vdrc.at).

Author Contributions

Conceptualization: Lanikea B. King, Seth M. Tomchik.

Data curation: Lanikea B. King.

Formal analysis: Lanikea B. King, Seth M. Tomchik.

Funding acquisition: James A. Walker, Seth M. Tomchik.

Investigation: Lanikea B. King, Tamara Boto, Valentina Botero, Ari M. Aviles, Breanna M. Jomsky, Chevara Joseph, James A. Walker.

Methodology: Lanikea B. King, Seth M. Tomchik.

Project administration: Seth M. Tomchik.

Resources: James A. Walker, Seth M. Tomchik.

Software: Seth M. Tomchik.

Supervision: Seth M. Tomchik.

Visualization: Lanikea B. King, James A. Walker, Seth M. Tomchik.

Writing – original draft: Lanikea B. King, Seth M. Tomchik.

Writing – review & editing: Lanikea B. King, Tamara Boto, Valentina Botero, Ari M. Aviles, Breanna M. Jomsky, Chevara Joseph, James A. Walker, Seth M. Tomchik.

References

1. Hyman SL, Shores A, North KN. (2005) The nature and frequency of cognitive deficits in children with neurofibromatosis type 1. *Neurology* 65: 1037–44. <https://doi.org/10.1212/01.wnl.0000179303.72345.ce> PMID: 16217056
2. Diggs-Andrews KA, Gutmann DH. (2013) Modeling cognitive dysfunction in neurofibromatosis-1. *Trends Neurosci* 36: 237–47. <https://doi.org/10.1016/j.tins.2012.12.002> PMID: 23312374
3. Constantino JN, Zhang Y, Holzhauser K, Sant S, Long K, Vallorani A, Malik L, Gutmann DH. (2015) Distribution and Within-Family Specificity of Quantitative Autistic Traits in Patients with Neurofibromatosis Type I. *J Pediatr* 167: 621–6 e1. <https://doi.org/10.1016/j.jpeds.2015.04.075> PMID: 26051969
4. Eijk S, Mous SE, Dieleman GC, Dierckx B, Rietman AB, de Nijs PFA, Ten Hoopen LW, van Minkelen R, Elgersma Y, Catsman-Berreoets CE, Oostenbrink R, Legerstee JS. (2018) Autism Spectrum Disorder in an Unselected Cohort of Children with Neurofibromatosis Type 1 (NF1). *J Autism Dev Disord*, <https://doi.org/10.1007/s10803-018-3478-0> PMID: 29423604
5. Garg S, Green J, Leadbitter K, Emsley R, Lehtonen A, Evans DG, Huson SM. (2013) Neurofibromatosis type 1 and autism spectrum disorder. *Pediatrics* 132: e1642–8. <https://doi.org/10.1542/peds.2013-1868> PMID: 24190681
6. Hyman SL, Shores EA, North KN. (2006) Learning disabilities in children with neurofibromatosis type 1: subtypes, cognitive profile, and attention-deficit-hyperactivity disorder. *Dev Med Child Neurol* 48: 973–7. <https://doi.org/10.1017/S0012162206002131> PMID: 17109785
7. Morris SM, Acosta MT, Garg S, Green J, Huson S, Legius E, North KN, Payne JM, Plasschaert E, Frazier TW, Weiss LA, Zhang Y, Gutmann DH, Constantino JN. (2016) Disease Burden and Symptom Structure of Autism in Neurofibromatosis Type 1: A Study of the International NF1-ASD Consortium Team (INFACT). *JAMA Psychiatry* 73: 1276–84. <https://doi.org/10.1001/jamapsychiatry.2016.2600> PMID: 27760236
8. Plasschaert E, Van Eylen L, Descheemaeker MJ, Noens I, Legius E, Steyaert J. (2016) Executive functioning deficits in children with neurofibromatosis type 1: The influence of intellectual and social functioning. *Am J Med Genet B Neuropsychiatr Genet* 171B: 348–62. <https://doi.org/10.1002/ajmg.b.32414> PMID: 26773288
9. Walsh KS, Velez JI, Kardel PG, Imas DM, Muenke M, Packer RJ, Castellanos FX, Acosta MT. (2013) Symptomatology of autism spectrum disorder in a population with neurofibromatosis type 1. *Dev Med Child Neurol* 55: 131–8. <https://doi.org/10.1111/dmnc.12038> PMID: 23163951
10. Payne JM. (2013) Autism spectrum disorder symptomatology in children with neurofibromatosis type 1. *Dev Med Child Neurol* 55: 100–1. <https://doi.org/10.1111/dmnc.12075> PMID: 23320572
11. Ozonoff S. (1999) Cognitive impairment in neurofibromatosis type 1. *Am J Med Genet* 89: 45–52. PMID: 10469436
12. Cichowski K, Jacks T. (2001) NF1 tumor suppressor gene function: narrowing the GAP. *Cell* 104: 593–604. [https://doi.org/10.1016/s0092-8674\(01\)00245-8](https://doi.org/10.1016/s0092-8674(01)00245-8) PMID: 11239415
13. Martin GA, Viskochil D, Bollag G, McCabe PC, Crosier WJ, Haubruck H, Conroy L, Clark R, O'Connell P, Cawthon RM, et al. (1990) The GAP-related domain of the neurofibromatosis type 1 gene product interacts with ras p21. *Cell* 63: 843–9. [https://doi.org/10.1016/0092-8674\(90\)90150-d](https://doi.org/10.1016/0092-8674(90)90150-d) PMID: 2121370
14. Oliveira AF, Yasuda R. (2014) Neurofibromin is the major ras inactivator in dendritic spines. *J Neurosci* 34: 776–83. <https://doi.org/10.1523/JNEUROSCI.3096-13.2014> PMID: 24431436
15. Brown JA, Gianino SM, Gutmann DH. (2010) Defective cAMP generation underlies the sensitivity of CNS neurons to neurofibromatosis-1 heterozygosity. *J Neurosci* 30: 5579–89. <https://doi.org/10.1523/JNEUROSCI.3994-09.2010> PMID: 20410111
16. The I, Hannigan GE, Cowley GS, Reginald S, Zhong Y, Gusella JF, Hariharan IK, Bernards A. (1997) Rescue of a *Drosophila* NF1 mutant phenotype by protein kinase A. *Science* 276: 791–4. <https://doi.org/10.1126/science.276.5313.791> PMID: 9115203
17. Walker JA, Gouzi JY, Long JB, Huang S, Maher RC, Xia H, Khalil K, Ray A, Van Vactor D, Bernards R, Bernards A. (2013) Genetic and functional studies implicate synaptic overgrowth and ring gland cAMP/PKA signaling defects in the *Drosophila melanogaster* neurofibromatosis-1 growth deficiency. *PLoS Genet* 9: e1003958. <https://doi.org/10.1371/journal.pgen.1003958> PMID: 24278035
18. Tong J, Hannan F, Zhu Y, Bernards A, Zhong Y. (2002) Neurofibromin regulates G protein-stimulated adenylyl cyclase activity. *Nat Neurosci* 5: 95–6. <https://doi.org/10.1038/nn792> PMID: 11788835

19. Xie K, Colgan LA, Dao MT, Muntean BS, Sutton LP, Orlandi C, Boye SL, Boye SE, Shih CC, Li Y, Xu B, Smith RG, Yasuda R, Martemyanov KA. (2016) NF1 Is a Direct G Protein Effector Essential for Opioid Signaling to Ras in the Striatum. *Curr Biol* 26: 2992–3003. <https://doi.org/10.1016/j.cub.2016.09.010> PMID: 27773571
20. Diggs-Andrews KA, Tokuda K, Izumi Y, Zorumski CF, Wozniak DF, Gutmann DH. (2013) Dopamine deficiency underlies learning deficits in neurofibromatosis-1 mice. *Ann Neurol* 73: 309–15. <https://doi.org/10.1002/ana.23793> PMID: 23225063
21. Wolman MA, de Groh ED, McBride SM, Jongsens TA, Granato M, Epstein JA. (2014) Modulation of cAMP and ras signaling pathways improves distinct behavioral deficits in a zebrafish model of neurofibromatosis type 1. *Cell Rep* 8: 1265–70. <https://doi.org/10.1016/j.celrep.2014.07.054> PMID: 25176649
22. Ryu HH, Lee YS. (2016) Cell type-specific roles of RAS-MAPK signaling in learning and memory: Implications in neurodevelopmental disorders. *Neurobiol Learn Mem* 135: 13–21. <https://doi.org/10.1016/j.nlm.2016.06.006> PMID: 27296701
23. Zhong J. (2016) RAS and downstream RAF-MEK and PI3K-AKT signaling in neuronal development, function and dysfunction. *Biol Chem* 397: 215–22. <https://doi.org/10.1515/hsz-2015-0270> PMID: 26760308
24. Bajenaru ML, Hernandez MR, Perry A, Zhu Y, Parada LF, Garbow JR, Gutmann DH. (2003) Optic nerve glioma in mice requires astrocyte Nf1 gene inactivation and Nf1 brain heterozygosity. *Cancer Res* 63: 8573–7. PMID: 14695164
25. Yang FC, Ingram DA, Chen S, Zhu Y, Yuan J, Li X, Yang X, Knowles S, Horn W, Li Y, Zhang S, Yang Y, Vakili ST, Yu M, Burns D, Robertson K, Hutchins G, Parada LF, Clapp DW. (2008) Nf1-dependent tumors require a microenvironment containing Nf1+/- and c-kit-dependent bone marrow. *Cell* 135: 437–48. <https://doi.org/10.1016/j.cell.2008.08.041> PMID: 18984156
26. Cui Y, Costa RM, Murphy GG, Elgersma Y, Zhu Y, Gutmann DH, Parada LF, Mody I, Silva AJ. (2008) Neurofibromin regulation of ERK signaling modulates GABA release and learning. *Cell* 135: 549–60. <https://doi.org/10.1016/j.cell.2008.09.060> PMID: 18984165
27. Sutton LP, Muntean BS, Ostrovskaya O, Zucca S, Dao M, Orlandi C, Song C, Xie K, Martemyanov KA. (2019) NF1-cAMP signaling dissociates cell type-specific contributions of striatal medium spiny neurons to reward valuation and motor control. *PLoS Biol* 17: e3000477. <https://doi.org/10.1371/journal.pbio.3000477> PMID: 31600280
28. Buchanan ME, Davis RL. (2010) A distinct set of Drosophila brain neurons required for neurofibromatosis type 1-dependent learning and memory. *J Neurosci* 30: 10135–43. <https://doi.org/10.1523/JNEUROSCI.0283-10.2010> PMID: 20668197
29. Walker JA, Tchoudakova AV, McKenney PT, Brill S, Wu D, Cowley GS, Hariharan IK, Bernards A. (2006) Reduced growth of Drosophila neurofibromatosis 1 mutants reflects a non-cell-autonomous requirement for GTPase-Activating Protein activity in larval neurons. *Genes Dev* 20: 3311–23. <https://doi.org/10.1101/gad.1466806> PMID: 17114577
30. King LB, Koch M, Murphy KR, Velazquez Y, Ja WW, Tomchik SM. (2016) Neurofibromin Loss of Function Drives Excessive Grooming in Drosophila. *G3 (Bethesda)* 6: 1083–93.
31. Hampel S, Franconville R, Simpson JH, Seeds AM. (2015) A neural command circuit for grooming movement control. *Elife* 4: e08758. <https://doi.org/10.7554/eLife.08758> PMID: 26344548
32. Namiki S, Dickinson MH, Wong AM, Korff W, Card GM. (2018) The functional organization of descending sensory-motor pathways in Drosophila. *Elife* 7.
33. Cande J, Namiki S, Qiu J, Korff W, Card GM, Shaevitz JW, Stern DL, Berman GJ. (2018) Optogenetic dissection of descending behavioral control in Drosophila. *Elife* 7.
34. Yellman C, Tao H, He B, Hirsh J. (1997) Conserved and sexually dimorphic behavioral responses to biogenic amines in decapitated Drosophila. *Proc Natl Acad Sci U S A* 94: 4131–6. <https://doi.org/10.1073/pnas.94.8.4131> PMID: 9108117
35. Hampel S, McKellar CE, Simpson JH, Seeds AM. (2017) Simultaneous activation of parallel sensory pathways promotes a grooming sequence in Drosophila. *Elife* 6.
36. Dietzl G, Chen D, Schnorrer F, Su KC, Barinova Y, Fellner M, Gasser B, Kinsey K, Oettel S, Scheiblauer S, Couto A, Marra V, Keleman K, Dickson BJ. (2007) A genome-wide transgenic RNAi library for conditional gene inactivation in Drosophila. *Nature* 448: 151–6. <https://doi.org/10.1038/nature05954> PMID: 17625558
37. Simpson JH. (2016) Rationally subdividing the fly nervous system with versatile expression reagents. *J Neurogenet* 30: 185–94. <https://doi.org/10.1080/01677063.2016.1248761> PMID: 27846759
38. Clyne JD, Miesenböck G. (2008) Sex-specific control and tuning of the pattern generator for courtship song in Drosophila. *Cell* 133: 354–63. <https://doi.org/10.1016/j.cell.2008.01.050> PMID: 18423205

39. Stowers RS. (2011) An efficient method for recombineering GAL4 and QF drivers. *Fly (Austin)* 5: 371–8.
40. Robb S, Cheek TR, Hannan FL, Hall LM, Midgley JM, Evans PD. (1994) Agonist-specific coupling of a cloned *Drosophila* octopamine/tyramine receptor to multiple second messenger systems. *EMBO J* 13: 1325–30. PMID: [8137817](#)
41. Ratner N, Miller SJ. (2015) A RASopathy gene commonly mutated in cancer: the neurofibromatosis type 1 tumour suppressor. *Nat Rev Cancer* 15: 290–301. <https://doi.org/10.1038/nrc3911> PMID: [25877329](#)
42. Guo HF, The I, Hannan F, Bernards A, Zhong Y. (1997) Requirement of *Drosophila* NF1 for activation of adenylyl cyclase by PACAP38-like neuropeptides. *Science* 276: 795–8. <https://doi.org/10.1126/science.276.5313.795> PMID: [9115204](#)
43. Guo HF, Tong J, Hannan F, Luo L, Zhong Y. (2000) A neurofibromatosis-1-regulated pathway is required for learning in *Drosophila*. *Nature* 403: 895–8. <https://doi.org/10.1038/35002593> PMID: [10706287](#)
44. Dasgupta B, Dugan LL, Gutmann DH. (2003) The neurofibromatosis 1 gene product neurofibromin regulates pituitary adenylate cyclase-activating polypeptide-mediated signaling in astrocytes. *J Neurosci* 23: 8949–54. <https://doi.org/10.1523/JNEUROSCI.23-26-08949.2003> PMID: [14523097](#)
45. Tong JJ, Schriener SE, McCleary D, Day BJ, Wallace DC. (2007) Life extension through neurofibromin mitochondrial regulation and antioxidant therapy for neurofibromatosis-1 in *Drosophila melanogaster*. *Nat Genet* 39: 476–85. <https://doi.org/10.1038/ng2004> PMID: [17369827](#)
46. Tsai PI, Wang M, Kao HH, Cheng YJ, Walker JA, Chen RH, Chien CT. (2012) Neurofibromin mediates FAK signaling in confining synapse growth at *Drosophila* neuromuscular junctions. *J Neurosci* 32: 16971–81. <https://doi.org/10.1523/JNEUROSCI.1756-12.2012> PMID: [23175848](#)
47. Klose A, Ahmadian MR, Schuelke M, Scheffzek K, Hoffmeyer S, Gewies A, Schmitz F, Kaufmann D, Peters H, Wittinghofer A, Nurnberg P. (1998) Selective disactivation of neurofibromin GAP activity in neurofibromatosis type 1. *Hum Mol Genet* 7: 1261–8. <https://doi.org/10.1093/hmg/7.8.1261> PMID: [9668168](#)
48. McGuire SE, Le PT, Osborn AJ, Matsumoto K, Davis RL. (2003) Spatiotemporal rescue of memory dysfunction in *Drosophila*. *Science* 302: 1765–8. <https://doi.org/10.1126/science.1089035> PMID: [14657498](#)
49. Ma Z, Stork T, Bergles DE, Freeman MR. (2016) Neuromodulators signal through astrocytes to alter neural circuit activity and behaviour. *Nature* 539: 428–32. <https://doi.org/10.1038/nature20145> PMID: [27828941](#)
50. Schutzler N, Girwert C, Hugli I, Mohana G, Roignant JY, Ryglewski S, Duch C. (2019) Tyramine action on motoneuron excitability and adaptable tyramine/octopamine ratios adjust *Drosophila* locomotion to nutritional state. *Proc Natl Acad Sci U S A* 116: 3805–10. <https://doi.org/10.1073/pnas.1813554116> PMID: [30808766](#)
51. Li HH, Kroll JR, Lennox SM, Ogundeyi O, Jeter J, Depasquale G, Truman JW. (2014) A GAL4 driver resource for developmental and behavioral studies on the larval CNS of *Drosophila*. *Cell Rep* 8: 897–908. <https://doi.org/10.1016/j.celrep.2014.06.065> PMID: [25088417](#)
52. Jenett A, Rubin GM, Ngo TT, Shepherd D, Murphy C, Dionne H, Pfeiffer BD, Cavallaro A, Hall D, Jeter J, Iyer N, Fetter D, Hausenfluck JH, Peng H, Trautman ET, Svirskas RR, Myers EW, Iwinski ZR, Aso Y, DePasquale GM, Enos A, Hulamm P, Lam SC, Li HH, Lavery TR, Long F, Qu L, Murphy SD, Rokicki K, Safford T, Shaw K, Simpson JH, Sowell A, Tae S, Yu Y, Zugates CT. (2012) A GAL4-driver line resource for *Drosophila* neurobiology. *Cell Rep* 2: 991–1001. <https://doi.org/10.1016/j.celrep.2012.09.011> PMID: [23063364](#)
53. Seeds AM, Ravbar P, Chung P, Hampel S, Midgley FM Jr., Mensh BD, Simpson JH. (2014) A suppression hierarchy among competing motor programs drives sequential grooming in *Drosophila*. *Elife* 3: e02951. <https://doi.org/10.7554/eLife.02951> PMID: [25139955](#)
54. Truman JW. (1990) Metamorphosis of the central nervous system of *Drosophila*. *J Neurobiol* 21: 1072–84. <https://doi.org/10.1002/neu.480210711> PMID: [1979610](#)
55. Truman JW. (2019) The Evolution of Insect Metamorphosis. *Curr Biol* 29: R1252–R68. <https://doi.org/10.1016/j.cub.2019.10.009> PMID: [31794762](#)
56. Lin S, Marin EC, Yang CP, Kao CF, Apenteng BA, Huang Y, O'Connor MB, Truman JW, Lee T. (2013) Extremes of lineage plasticity in the *Drosophila* brain. *Curr Biol* 23: 1908–13. <https://doi.org/10.1016/j.cub.2013.07.074> PMID: [24055154](#)
57. Maysseless O, Berns DS, Yu XM, Riemensperger T, Fiala A, Schuldiner O. (2018) Developmental Coordination during Olfactory Circuit Remodeling in *Drosophila*. *Neuron* 99: 1204–15 e5. <https://doi.org/10.1016/j.neuron.2018.07.050> PMID: [30146303](#)

58. Sopko R, Perrimon N. (2013) Receptor tyrosine kinases in *Drosophila* development. *Cold Spring Harb Perspect Biol* 5.
59. Lee HH, Norris A, Weiss JB, Frasch M. (2003) Jelly belly protein activates the receptor tyrosine kinase Alk to specify visceral muscle pioneers. *Nature* 425: 507–12. <https://doi.org/10.1038/nature01916> PMID: 14523446
60. Bazigou E, Apitz H, Johansson J, Loren CE, Hirst EM, Chen PL, Palmer RH, Salecker I. (2007) Anterograde Jelly belly and Alk receptor tyrosine kinase signaling mediates retinal axon targeting in *Drosophila*. *Cell* 128: 961–75. <https://doi.org/10.1016/j.cell.2007.02.024> PMID: 17350579
61. Rohrbough J, Broadie K. (2010) Anterograde Jelly belly ligand to Alk receptor signaling at developing synapses is regulated by Mind the gap. *Development* 137: 3523–33. <https://doi.org/10.1242/dev.047878> PMID: 20876658
62. Rohrbough J, Kent KS, Broadie K, Weiss JB. (2013) Jelly Belly trans-synaptic signaling to anaplastic lymphoma kinase regulates neurotransmission strength and synapse architecture. *Dev Neurobiol* 73: 189–208. <https://doi.org/10.1002/dneu.22056> PMID: 22949158
63. Walker JA, Bernards A. (2014) A *Drosophila* screen identifies neurofibromatosis-1 genetic modifiers involved in systemic and synaptic growth. *Rare Dis* 2: e28341. <https://doi.org/10.4161/rdis.28341> PMID: 25054093
64. Simon MA, Bowtell DD, Dodson GS, Lavery TR, Rubin GM. (1991) Ras1 and a putative guanine nucleotide exchange factor perform crucial steps in signaling by the sevenless protein tyrosine kinase. *Cell* 67: 701–16. [https://doi.org/10.1016/0092-8674\(91\)90065-7](https://doi.org/10.1016/0092-8674(91)90065-7) PMID: 1934068
65. Li W, Cui Y, Kushner SA, Brown RA, Jentsch JD, Frankland PW, Cannon TD, Silva AJ. (2005) The HMG-CoA reductase inhibitor lovastatin reverses the learning and attention deficits in a mouse model of neurofibromatosis type 1. *Curr Biol* 15: 1961–7. <https://doi.org/10.1016/j.cub.2005.09.043> PMID: 16271875